

Triadic interactions induce blinking and chaos in the connectivity of higher-order networks

Hanlin Sun,¹ Filippo Radicchi,² Juergen Kurths,^{3,4} and Ginestra Bianconi^{1,5}

¹*School of Mathematical Sciences, Queen Mary University of London, London, E1 4NS, United Kingdom*

²*Center for Complex Networks and Systems Research, Luddy School of Informatics, Computing, and Engineering, Indiana University, Bloomington, 47408, USA*

³*Potsdam Institute for Climate Impact Research, Potsdam, Germany*

⁴*Department of Physics, Humboldt University of Berlin, Berlin, Germany*

⁵*The Alan Turing Institute, The British Library, London*

Ecological, biochemical and neuronal networks are characterized by triadic interactions formed by one node regulating the interaction between two other nodes. However, little is known about the effect of triadic interactions on macroscopic network properties. Here, we show that the combination of positive and negative regulatory interactions turns percolation into a fully-fledged dynamical system where the giant connected component intermittently involves a different set of nodes, and the order parameter undergoes period doubling and a route to chaos. This phenomenon is captured by a theory validated by numerical simulations on both synthetic and real networks.

Higher-order networks are ubiquitous in nature [1–6]. Paradigmatic examples are brain and chemical reaction networks [7–9]. Higher-order interactions may profoundly change the physical properties of a dynamical process compared to those displayed by the same process occurring on a classic network of pairwise interactions. Examples include synchronization [10–13], random walk dynamics [14], contagion dynamics [15–20] and game theory [21].

In this paper, we focus on a specific type of higher-order interactions named triadic interactions. A triadic interaction describes the regulatory activity of a node on the link between two other nodes. Regulation can be either positive, in the sense that the node facilitates the interaction, or negative, meaning that the regulator inhibits the interaction. Triadic interactions occur in ecosystems, where the competition between two species can be affected by the presence of a third species [22–24]. In chemical reaction networks, enzymes act as biological catalysts for reactions. In brain networks, the synaptic interaction between neurons is modulated by glias [25].

To the best of our knowledge, theoretical analyses of triadic interactions have been considered so far only for investigating small-scale dynamical systems describing species' abundance in ecological networks [22–24].

Here, we change perspective and study the role of triadic interactions in shaping macroscopic network properties. We show that the large-scale connectivity of a higher-order network with triadic interactions is characterized by a time-dependent order parameter that undergoes period doubling and a route to chaos. We therefore establish a clear connection between non-linear dynamics on networks [26–28] and the percolation transition [29]. In particular, we show how the presence of triadic interactions turns bond percolation into a fully-fledged dynamical process.

Bond-percolation describe how the failure of some of the network edges affects the macroscopic connectivity

of the system [30]. Being connected is a necessary condition for interaction, therefore percolation models allow for the establishment of the minimal requirements that a network should satisfy in order to support any type of interactive process that may occur on the network. In the ordinary version of the model, individual edges fail with probability $q = 1 - p$. Depending on the value of such a probability, the network can be found in two phases: (i) the percolating phase, where a single giant connected component (GC) exists in the network, and (ii) the non-percolating phase, where the network is composed of non-extensive connected components only. The model is a pivotal example for critical phenomena on networks [29]. On simple networks, it displays a continuous, second-order phase transition. Several papers of the last decade consider possible variants of the model leading to discontinuous, first-order phase transitions [31–39]. On multilayer networks [40–42], percolation displays a discontinuous hybrid transition [36, 43–46]. In the context of multilayer networks, some attention has also been addressed to competitive or antagonistic interactions [47–49] among the different layers of the multiplex networks leading to bistability of the stationary state of the percolation process [47].

In this work, we propose a dynamical model of percolation that explicitly accounts for triadic interactions. The model consists of an iterative percolation-regulation procedure, where the two processes are applied in sequence and the outcome of one process influences the outcome of the other. The percolation-regulation scheme is possible under the assumption of a separation of time scales between the two interacting processes, with regulation taking place on a time scale much longer than the one of percolation. We study the model on both real and synthetic network topologies finding a universal set of results. If only positive regulatory interactions are allowed, then the dynamical model always reaches a steady state. In particular, we find that the size of the giant connect

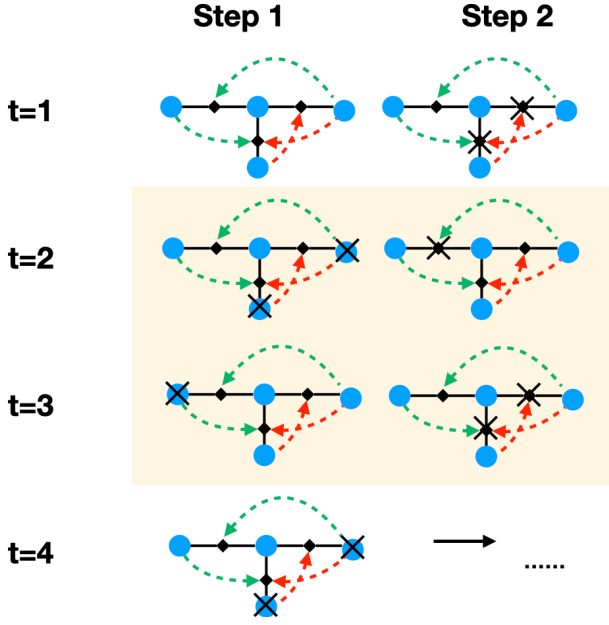


FIG. 1. Sketch of the dynamically regulated percolation on higher-order network with triadic interactions. Solid lines represent structural links, dashed curves denotes regulatory interactions (green stands for positive regulation, red for negative). Blue filled circles indicate structural nodes, black diamonds indicate triadic interactions. For simplicity, we consider the deterministic bond-percolation model for $p = p_0 = 1$. At each stage t of the dynamics, bond percolation is applied to the network, and then the effect of the regulatory activity is established. The illustration shows how the dynamics sets into a periodic pattern with the node activities “blinking” in time. The periodic pattern is highlighted in yellow. At time $t = 1$, all links are intact and all nodes are part of the giant component (GC). Their regulatory activity causes some links to become inactive (crossed links in the figure). As a consequence, at time $t = 2$, some nodes are no longer part of the GC and become inactive (crossed nodes in the figure). However, this change leads to changes in the state of some links, which in turn affect the state of the nodes at time $t = 3, 4$, etc. The final configuration reached at time $t = 3$ is identical to one observed at end of stage $t = 1$. Due to the determinism of the model, the pattern repeats with period $T = 2$. The relative size R of the GC oscillates switches between $2/4$ and $3/4$.

component of the network undergoes a discontinuous and hybrid phase transition, as in the case of ordinary percolation on multilayer networks. However, in presence of both positive and negative regulatory interactions instead, the model displays a rich dynamical behavior with period doubling and a route to chaos. We provide evidence of these findings by means of extensive numerical simulations and an approximate analytical treatment of the model.

Model- We envision our higher-order network as composed of two networks: the structural network and the regulatory network. The structural network $\mathcal{A} = (V, E)$ is formed by the set of nodes V connected by the struc-

tural links in the set E . The regulatory network $\mathcal{B} = (V, E, W)$ is a bipartite, signed network between the set of nodes V of the structural network and the set of structural links E , with nodes in V regulating links in E on the basis of the regulatory interactions, either positive or negative, specified in the set W .

We consider a model in which the activity of nodes and links is changing in time due to the triadic regulatory interactions of links and due to connectivity considerations leading to a regulated percolation process. At time $t = 0$, every structural link is damaged with probability $q_0 = 1 - p_0$. We then iterate the following algorithm for each time step $t \geq 1$:

Step 1 Given a certain damage of the structural links happened at time $t - 1$, we set as *active* the state of all nodes in the giant component of the structural network and as *inactive* all the other nodes of the network.

Step 2 Given the set of all active nodes obtained in step 1, we damage all links that are connected at least to one active negative regulator node and/or that are not connected to any active positive regulator node. All the other links are damaged with probability $q = 1 - p$.

Note that for $p = p_0 = 1$ the model is deterministic. However, for $p < 1$ the model is stochastic as the Step 2 retains a stochastic character.

Figure 1 illustrates a typical realization of the model. Already there, one can appreciate how in a typical realization of this model the presence of triadic interactions can lead to a non-trivial dynamics characterized by network “blinking,” with nodes turning on and off periodically to form GCs of different size.

The various choices made in the design of the model are certainly simplistic and arbitrary. However, they can all be supported by some reasonable arguments. Specifically, the assumption that only nodes within the GC of the network are considered functioning/active is well accepted in the literature concerning network robustness [29]. Also, we do not expect the general behavior of the model to be too sensitive to the specific choice of the threshold for positive/negative regulations made here. Finally, the underlying ordinary percolation model represents a simple way to account for the unavoidable randomness that should affect both structural and regulatory networks in the real world.

Networks - We assume that the structural network \mathcal{A} is given and contains N nodes and $\langle k \rangle N$ structural links, with $\langle k \rangle$ average degree of the network. We consider structural networks given by individual instances of the configuration model [50]. To this end, we first generate degree sequences by selecting random variables from either Poisson or power-law degree distributions $\pi(k)$. Also, we consider real-world structural networks constructed from empirical data collected by Ref. [51].

To generate the regulatory network \mathcal{B} , we assume that every node i has associated two degree values, namely the number of positive regulatory interactions κ_i^+ , and the number of negative regulatory interactions κ_i^- . For simplicity we consider the case in which both κ_i^+ and κ_i^- are chosen independently on the structural degree k . Each structural link ℓ is assigned the degrees $\hat{\kappa}_\ell^+$ and $\hat{\kappa}_\ell^-$ indicating the number of positive regulators and the number of negative regulators, respectively. In particular, nodes' degrees are extracted at random from the distribution $P(\kappa^+, \kappa^-)$, and links' degrees are randomly extracted from the distribution $\hat{P}_+(\hat{\kappa}^+)\hat{P}_-(\hat{\kappa}^-)$. Once degrees have been assigned to nodes and links, we establish the existence of a positive + or negative - regulatory interaction between the structural link ℓ and the node i with probability

$$p_{\ell,i}^\pm = \frac{\kappa_i^\pm \hat{\kappa}_\ell^\pm}{\langle \kappa^\pm \rangle N}, \quad (1)$$

where $\langle \kappa^\pm \rangle$ denotes the average of κ over all the nodes of the network.

Theory- Here we provide the theory for regulated percolation in the considered uncorrelated scenario in which the degree of a node in the structural network is independent on its degrees in the regulatory network (see the SM for the extension to the correlated case). If the structural network \mathcal{A} is generated according to the configuration model, and the network is sufficiently large and sparse, solutions of the model described above can be well approximated by the following analytical treatment that combines the theory of percolation with the theory of dynamical systems. Let us define $S^{(t)}$ as the probability that a node at the endpoint of a random structural link of network \mathcal{A} is in the GC at time t . $R^{(t)\pm}$ indicates instead the fraction of the nodes in the GC at time t or equivalently the probability that a node at the end of a regulatory link is active. Finally, $p_L^{(t)}$ is the probability that a random node is damaged at time t . By putting $p_L^{(0)} = p_0$ indicating the probability that structural links are damaged at time $t = 0$, we have that for $t > 0$, as long as the network is locally tree like, $S^{(t)}$, $R^{(t)}$ and $p_L^{(t)}$ are updated as

$$\begin{aligned} S^{(t)} &= 1 - G_1 \left(1 - S^{(t)} p_L^{(t-1)} \right), \\ R^{(t)} &= 1 - G_0 \left(1 - S^{(t)} p_L^{(t-1)} \right), \\ p_L^{(t)} &= p G_0^- (1 - R^{(t)}) \left[1 - G_0^+ \left(1 - R^{(t)} \right) \right], \end{aligned} \quad (2)$$

where

$$\begin{aligned} G_0(x) &= \sum_k \pi(k) x^k, \\ G_1(x) &= \sum_k \pi(k) \frac{k}{\langle k \rangle} x^{k-1}, \\ G_0^\pm(x) &= \sum_{\kappa_\pm} \hat{P}_\pm(\hat{\kappa}_\pm) x^{\hat{\kappa}_\pm}. \end{aligned} \quad (3)$$

The Eq. (2) for the percolation model regulated by triadic interactions can be formally written as the map [52]:

$$R^{(t)} = f \left(p_L^{(t-1)} \right), \quad (4)$$

$$p_L^{(t)} = g_p \left(R^{(t)} \right). \quad (5)$$

The previous sets of equations can be numerically integrated to generate approximate solutions valid for structural networks generated according to the configuration model. Specifically, we note that $G_0(x)$ and $G_1(x)$ are the generating functions of, respectively, the degree distribution $\pi(k)$ and the excess degree distribution $\pi(k)k/\langle k \rangle$. These generating function appear in theoretical approximations of the percolation transition for simple networks [29]. The above framework differs from the traditional one defined on classical pairwise networks because of the presence of the regulatory network, whose contribution is summarized in the generating functions $G_0^\pm(x)$.

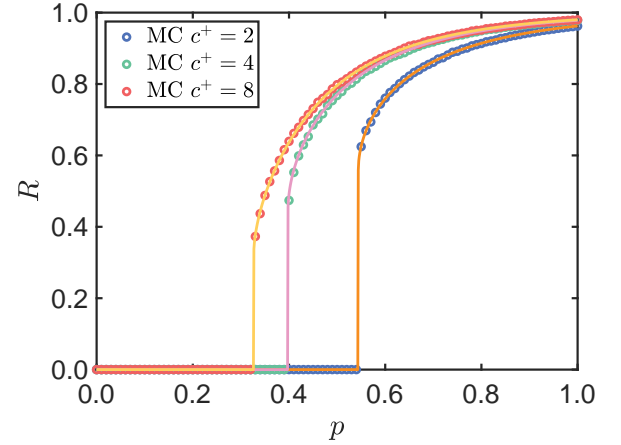


FIG. 2. The steady state value of the size R of the giant component as a function of the bond occupation probability p . We consider a Poisson structural network with average degree $c = 4$, and a Poisson distribution with average c^+ for the number of positive regulators $\hat{\kappa}^+$ per link. Here negative regulatory interactions are not present. The results obtained from Monte Carlo (MC) simulations (symbols) over networks of $N = 10^4$ nodes are compared to theoretical expectations (solid curves).

Results- In absence of negative triadic interactions, when all regulatory interactions are positive, the dynamics always reaches a stationary point with $R^{(t)} = R^*$, independent of time. In Figure 2 we show the dependent of this stationary state with p , i.e. $R^* = R^*(p)$. The agreement between theoretical predictions and results of numerical simulations is excellent. Interestingly, the order parameter R^* displays a discontinuous hybrid phase transition as a function of p showing that positive triadic interactions induce discontinuous hybrid percolation in

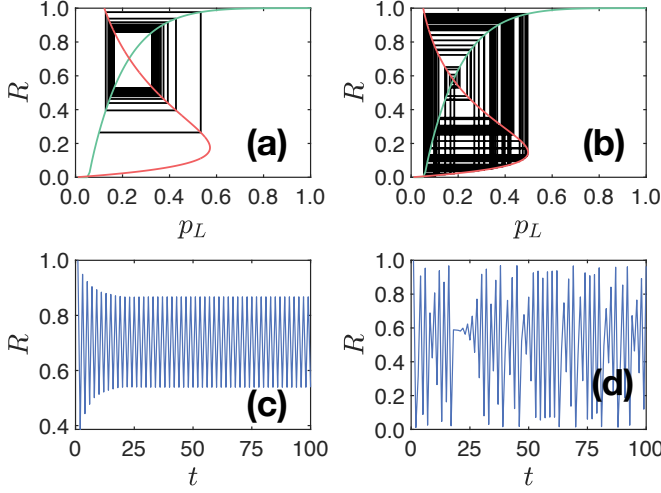


FIG. 3. (a) Theoretical cobweb of dynamically regulated percolation in presence of triadic interactions [Eqs. (4) (red) and Eq. (5) (green)]. The structural network has a power-law degree distribution $\pi(k) \sim k^{-\gamma}$, with minimum degree $m = 4$, maximum degree $K = 100$, and degree exponent $\gamma = 2.5$. $\hat{\kappa}^+$ and $\hat{\kappa}^-$ obeys Poisson distributions with average c^+ and c^- respectively with $c^+ = 10$ and $c^- = 2.1$, respectively. (b) Same as in a, but with $c^+ = 10$ and $c^- = 2.97$. (c) Relative size of the R as a function of time t . Results are obtained via MC simulations on a network instance with $N = 10^4$ and same parameters as in panel (a). (d) Same as in panel (c), but for a network generated with the same parameters as in panel (b).

higher-order networks (see Figure 2 and the analytical derivation in the SM).

In presence of negative interactions, the model is even more interesting as the dynamics of the percolation process we have defined undergoes a period doubling and a route to chaos for both Poisson networks and scale-free networks. The phenomenon reveals the emergence of both “blinking” oscillations and a chaotic pattern of the order parameter (see Figure 3). “Blinking” refers to the intermittent switching on and off of two or more sets of nodes leads to periodic oscillations or the order parameter (Figure 3(c)), chaos implies that at each time a different set of nodes (of different number of nodes) is activated (Figure 3(d)). The map of Eqs. (4) and (5) allows us to generate the cobweb of the dynamical process. Theoretical predictions display excellent agreement with results from extensive simulations of the model.

The bifurcation diagrams of Figure 4 reveal that the combination of negative and positive regulatory activity leads to a much richer behavior than to the one obtained in the case of positive regulation only, i.e., Figure 2. In this analysis, we monitor the relative size R of the GC as a function of the bond occupation probability p . Eqs. (4) and (5) predict period doubling and a route to chaos irrespective of the degree distribution of

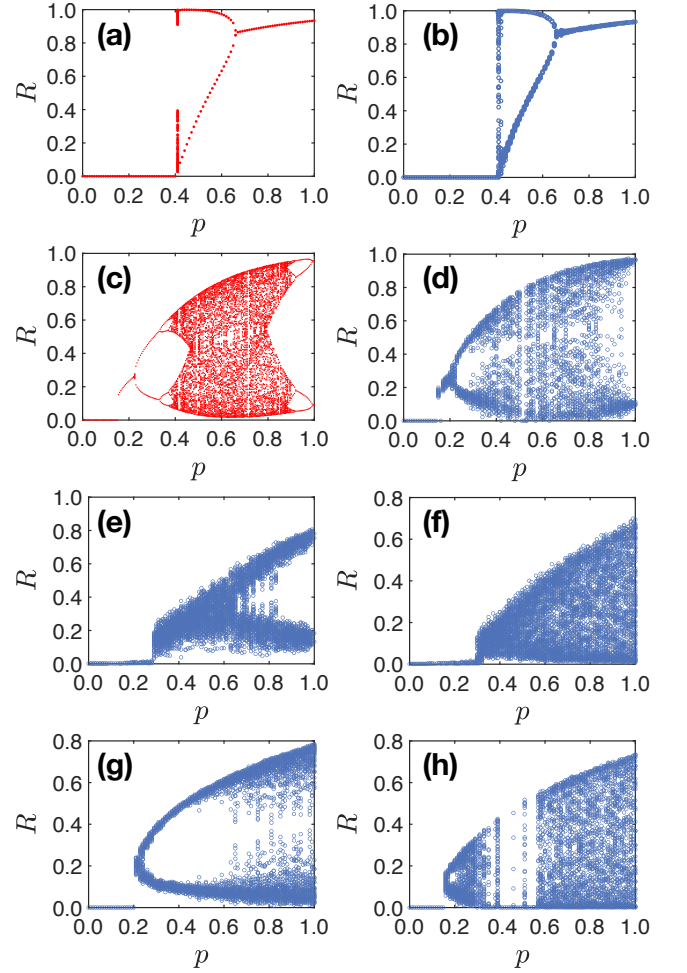


FIG. 4. Relative size R of the GC as a function of the bond occupation probability p display a route to chaos in percolation regulated by triadic interactions. The figure displays the solutions of Eqs. (2) for a Poisson structural network with average degree $c = 30$, and Poisson regulatory network with averages $c^+ = 10$ and $c^- = 2.5$. (b) Same as in panel (a), but obtained via Monte Carlo (MC) simulations on a network with size $N = 10^5$. Here and in all other panels concerning MC results, points represent all R values observed in the time range $150 \leq t \leq 200$. (c) Same as in (a), but for a structural scale-free graph with degree exponent $\gamma = 2.5$, minimum degree $m = 4$ and maximum degree $K = 100$. The regulatory network has a Poisson distribution with parameters $c^+ = 10$ and $c^- = 2.5$. (d) Same as in panel (c), but obtained via MC on a network with size $N = 10^4$. (e) Results of MC on the network mouse brain network [51]. The regulatory network has a Poisson distribution with parameters $c^+ = 20$ and $c^- = 2$. (f) Same as in (e), but with $c^+ = 20$ and $c^- = 4$ (f). (g) Same as in (e), but for the Human bio grid network [51], with $c^+ = 20$ and $c^- = 4$. (h) Same as in (g), but for $c^+ = 20$ and $c^- = 6$. All orbit diagrams are obtained with an initial condition $p_L^{(0)} = 0.1$.

the structural network (Figs .4a and .4c). Theoretical predictions are well matched by results of numerical simulations (Figs .4b and .4d). Although our theory does

allow to well approximate the dynamical behavior of the percolation model only for structural networks that are generated according to specific network models, results of numerical simulations clearly denote a rich dynamical behavior of the model also if structural networks are taken from the real world (Figs .4e-h).

Conclusions- A combination of positive and negative/antagonistic interactions is known to affect statistical mechanics problems in non-trivial ways [53, 54]. Here, we show that positive and negative regulatory triadic interactions can turn percolation into a fully dynamical process whose order parameter undergoes a period doubling and a route to chaos. In absence of negative regulatory interactions, this percolation process always reaches a steady state and the phase diagram displays a discontinuous hybrid phase transition.

The proposed framework can be applied to other generalized network structures such as hypergraphs and multiplex networks. Moreover the approach can be extended to situations in which the nodes sustain a more complex dynamics.

This research utilized Queen Mary's Apocrita HPC facility, supported by QMUL Research-IT. <http://doi.org/10.5281/zenodo.438045>. G.B. acknowledges support from the Royal Society (IEC\NSFC\191147. H.S. acknowledges support by the Chinese Scholarship Council. F.R. acknowledges support by the Air Force Office of Scientific Research (FA9550-21-1-0446) and the Army Research Office (W911NF-21-1-0194). The funders had no role in study design, data collection and analysis, decision to publish, or any opinions, findings, and conclusions or recommendations expressed in the manuscript. J.K. has been supported by the Alexander von Humboldt Polish Honorary Research Scholarship 2020 of the Fundation for Polish Science.

-
- [1] F. Battiston, G. Cencetti, I. Iacopini, V. Latora, M. Lucas, A. Patania, J.-G. Young, and G. Petri, *Physics Reports* **874**, 1 (2020).
 - [2] G. Bianconi, *Higher-order networks: An Introduction to Simplicial Complexes* (Cambridge University Press, 2021).
 - [3] S. Majhi, M. Perc, and D. Ghosh, *Journal of the Royal Society Interface* **19**, 20220043 (2022).
 - [4] V. Salnikov, D. Cassese, and R. Lambiotte, *European Journal of Physics* **40**, 014001 (2018).
 - [5] C. Bick, E. Gross, H. A. Harrington, and M. T. Schaub, *arXiv preprint arXiv:2104.11329* (2021).
 - [6] L. Torres, A. S. Blevins, D. Bassett, and T. Eliassi-Rad, *SIAM Review* **63**, 435 (2021).
 - [7] C. Giusti, R. Ghrist, and D. S. Bassett, *Journal of computational neuroscience* **41**, 1 (2016).
 - [8] J. Faskowitz, R. F. Betzel, and O. Sporns, *Network Neuroscience* **6**, 1 (2022).
 - [9] J. Jost and R. Mulas, *Advances in mathematics* **351**, 870 (2019).
 - [10] A. P. Millán, J. J. Torres, and G. Bianconi, *Physical Review Letters* **124**, 218301 (2020).
 - [11] P. S. Skardal and A. Arenas, *Physical review letters* **122**, 248301 (2019).
 - [12] Y. Zhang, V. Latora, and A. E. Motter, *Communications Physics* **4**, 1 (2021).
 - [13] R. Mulas, C. Kuehn, and J. Jost, *Physical Review E* **101**, 062313 (2020).
 - [14] T. Carletti, F. Battiston, G. Cencetti, and D. Fanelli, *Physical review E* **101**, 022308 (2020).
 - [15] G. St-Onge, H. Sun, A. Allard, L. Hébert-Dufresne, and G. Bianconi, *Physical Review Letters* **127**, 158301 (2021).
 - [16] G. F. de Arruda, G. Petri, and Y. Moreno, *Physical Review Research* **2**, 023032 (2020).
 - [17] I. Iacopini, G. Petri, A. Barrat, and V. Latora, *Nature communications* **10**, 1 (2019).
 - [18] G. Ferraz de Arruda, M. Tizzani, and Y. Moreno, *Communications Physics* **4**, 1 (2021).
 - [19] H. Sun and G. Bianconi, *Physical Review E* **104**, 034306 (2021).
 - [20] D. Taylor, F. Klimm, H. A. Harrington, M. Kramár, K. Mischaikow, M. A. Porter, and P. J. Mucha, *Nature communications* **6**, 1 (2015).
 - [21] U. Alvarez-Rodriguez, F. Battiston, G. F. de Arruda, Y. Moreno, M. Perc, and V. Latora, *Nature Human Behaviour* **5**, 586 (2021).
 - [22] E. Bairey, E. D. Kelsic, and R. Kishony, *Nature communications* **7**, 1 (2016).
 - [23] J. Grilli, G. Barabás, M. J. Michalska-Smith, and S. Allesina, *Nature* **548**, 210 (2017).
 - [24] A. D. Letten and D. B. Stouffer, *Ecology letters* **22**, 423 (2019).
 - [25] W.-H. Cho, E. Barcelon, and S. J. Lee, *Experimental neurobiology* **25**, 197 (2016).
 - [26] A. Arenas, A. Díaz-Guilera, J. Kurths, Y. Moreno, and C. Zhou, *Physics reports* **469**, 93 (2008).
 - [27] N. Marwan, J. F. Donges, Y. Zou, R. V. Donner, and J. Kurths, *Physics Letters A* **373**, 4246 (2009).
 - [28] M. A. Porter and J. P. Gleeson, *Frontiers in Applied Dynamical Systems: Reviews and Tutorials* **4** (2016).
 - [29] S. N. Dorogovtsev, A. V. Goltsev, and J. F. Mendes, *Reviews of Modern Physics* **80**, 1275 (2008).
 - [30] D. Stauffer and A. Aharony, *Introduction to percolation theory* (CRC press, 1992).
 - [31] R. M. D'Souza, J. Gómez-Gardenes, J. Nagler, and A. Arenas, *Advances in Physics* **68**, 123 (2019).
 - [32] D. Achlioptas, R. M. D'Souza, and J. Spencer, *science* **323**, 1453 (2009).
 - [33] O. Riordan and L. Warnke, *Science* **333**, 322 (2011).
 - [34] R. A. da Costa, S. N. Dorogovtsev, A. V. Goltsev, and J. F. F. Mendes, *Physical review letters* **105**, 255701 (2010).
 - [35] J. Fan, J. Meng, Y. Liu, A. A. Saberi, J. Kurths, and J. Nagler, *Nature Physics* **16**, 455 (2020).
 - [36] S. V. Buldyrev, R. Parshani, G. Paul, H. E. Stanley, and S. Havlin, *Nature* **464**, 1025 (2010).
 - [37] B. Min, S. Do Yi, K.-M. Lee, and K.-I. Goh, *Physical Review E* **89**, 042811 (2014).
 - [38] Y. S. Cho, J. S. Kim, J. Park, B. Kahng, and D. Kim, *Physical review letters* **103**, 135702 (2009).
 - [39] S. Boettcher, V. Singh, and R. M. Ziff, *Nature commu-*

- nications **3**, 1 (2012).
- [40] G. Bianconi, *Multilayer networks: structure and function* (Oxford university press, 2018).
 - [41] S. Boccaletti, G. Bianconi, R. Criado, C. I. Del Genio, J. Gómez-Gardenes, M. Romance, I. Sendina-Nadal, Z. Wang, and M. Zanin, *Physics reports* **544**, 1 (2014).
 - [42] M. Kivelä, A. Arenas, M. Barthélemy, J. P. Gleeson, Y. Moreno, and M. A. Porter, *Journal of complex networks* **2**, 203 (2014).
 - [43] G. Baxter, S. Dorogovtsev, A. Goltsev, and J. Mendes, *Physical review letters* **109**, 248701 (2012).
 - [44] F. Radicchi, *Nature Physics* **11**, 597 (2015).
 - [45] F. Radicchi and G. Bianconi, *Physical Review X* **7**, 011013 (2017).
 - [46] S. D. Reis, Y. Hu, A. Babino, J. S. Andrade Jr, S. Canals, M. Sigman, and H. A. Makse, *Nature Physics* **10**, 762 (2014).
 - [47] K. Zhao and G. Bianconi, *Journal of Statistical Mechanics: Theory and Experiment* **2013**, P05005 (2013).
 - [48] M. M. Danziger, I. Bonamassa, S. Boccaletti, and S. Havlin, *Nature Physics* **15**, 178 (2019).
 - [49] L. M. Shekhtman, M. M. Danziger, and S. Havlin, *Chaos, Solitons & Fractals* **90**, 28 (2016).
 - [50] M. Molloy and B. Reed, *Random structures & algorithms* **6**, 161 (1995).
 - [51] R. A. Rossi and N. K. Ahmed, in *Proceedings of the Twenty-Ninth AAAI Conference on Artificial Intelligence* (2015).
 - [52] S. H. Strogatz, *Nonlinear dynamics and chaos: with applications to physics, biology, chemistry, and engineering* (CRC press, 2018).
 - [53] M. Mézard, G. Parisi, and M. A. Virasoro, *Spin glass theory and beyond: An Introduction to the Replica Method and Its Applications*, Vol. 9 (World Scientific Publishing Company, 1987).
 - [54] A. E. Motter and M. Timme, *Annual review of condensed matter physics* **9**, 463 (2018).

SUPPLEMENTAL MATERIAL

REGULATED PERCOLATION FOR CORRELATED STRUCTURAL AND REGULATORY NETWORKS

General theoretical framework

In this appendix we extend the theoretical approach described in the main text in order to treat also the case in which the structural degree k of a node can be correlated with its regulatory degrees κ^+ and κ^- .

In this case the random higher-order network with triadic interactions is characterized by a joint degree distribution $\tilde{P}(k, \kappa^+, \kappa^-)$ and by the degree distributions $\hat{P}_\pm(\hat{\kappa}^\pm)$. The distribution $\tilde{P}(k, \kappa^+, \kappa^-)$ indicates the probability that a random node has structural degree k and regulatory degrees κ^+ and κ^- . The distributions $\hat{P}_\pm(\hat{\kappa}^\pm)$ indicate the probability that a random link has $\hat{\kappa}^+$ or $\hat{\kappa}^-$ regulatory interactions, respectively.

Let us define $S^{(t)}$ as the probability that a node at the endpoint of a random structural link of network \mathcal{A} is in the giant component (GC) at time t . Let us define $\hat{S}^{(t)\pm}$ as the probability that a node regulating (positively $+$ or negatively $-$) a random structural link is in the GC at time t . Let us define with $p_L^{(t)}$ the probability that a random node is damaged at time t . By putting $p_L^{(0)} = p_0$ indicating the probability that structural links are damaged at time $t = 0$, we have that for all $t > 0$, as long as the network is locally tree-like, $S^{(t)}$, $\hat{S}^{(t)\pm}$ and $p_L^{(t)}$ are updated as

$$\begin{aligned} S^{(t)} &= 1 - G_1 \left(1 - S^{(t)} p_L^{(t-1)}, \right) \\ \hat{S}^{(t)\pm} &= 1 - \mathcal{G}^\pm (1 - S^{(t)} p_L^{(t-1)}), \\ p_L^{(t)} &= p G_0^- (1 - \hat{S}^{(t)-}) \left[1 - G_0^+ (1 - \hat{S}^{(t)+}) \right], \end{aligned} \quad (\text{S-1})$$

where

$$\begin{aligned} G_1(x) &= \sum_{k, \kappa^+, \kappa^-} \tilde{P}(k, \kappa^+, \kappa^-) \frac{k}{\langle k \rangle} x^{k-1}, \\ G_0^\pm(x) &= \sum_{\kappa^\pm} \hat{P}_\pm(\hat{\kappa}^\pm) x^{\hat{\kappa}^\pm}, \\ \mathcal{G}^\pm(x) &= \sum_{k, \kappa^+, \kappa^-} \tilde{P}(k, \kappa^+, \kappa^-) \frac{\kappa^\pm}{\langle \kappa^\pm \rangle} x^{\kappa^\pm}. \end{aligned} \quad (\text{S-2})$$

The probability that a node is in the GC is given by

$$R^{(t)} = 1 - G_0 \left(1 - S^{(t)} p_L^{(t-1)} \right), \quad (\text{S-3})$$

where

$$G_0(x) = \sum_{k, \kappa^+, \kappa^-} \tilde{P}(k, \kappa^+, \kappa^-) x^k. \quad (\text{S-4})$$

The stationary solution and the onset of its instability

The equation for percolation regulated by triadic interaction can be formally written as a map [52]:

$$\hat{S}^{(t)\pm} = f^\pm(p_L^{(t-1)}), \quad p_L^{(t)} = g_p(\hat{S}^{(t),+}, \hat{S}^{(t)-}), \quad (\text{S-5})$$

whose stationary fixed point $\hat{S}^{\star\pm}, p_L^\star$ satisfies

$$\hat{S}^{\star\pm} = f^\pm(g_p(\hat{S}^{\star,+}, \hat{S}^{\star-})), \quad (\text{S-6})$$

or equivalently

$$p_L^\star = g_p(f^+(p_L^\star), f^-(p_L^\star)). \quad (\text{S-7})$$

The stationary solution becomes unstable when

$$|J| = 1, \quad (\text{S-8})$$

where

$$J = \left. \frac{dg_p(f^+(p_L), f^-(p_L))}{dp_L} \right|_{p_L=p_L^\star}. \quad (\text{S-9})$$

As we will show in the next paragraphs, there are two major types of instability. The first type of instability is observed when $J = 1$ and leads to discontinuous hybrid transitions. This type of instability is observed for instance in regulated percolation in absence of negative interactions. The second type of instability is achieved instead when $J = -1$ and this leads typically to the onset of period 2 oscillations of the order parameter $R^{(t)}$ of percolation.

Note that the stability of the periodic oscillations of the order parameter can be studied in an analogous way by investigating the stability of the map iterated for a number of times equal to the period of the oscillation under study. However, we leave this analysis to later works.

Limiting case of uncorrelated structural and regulatory degrees of the nodes

If we assume that the structural and regulatory degrees of the nodes are uncorrelated, we can then write

$$\tilde{P}(k, \kappa^+, \kappa^-) = \pi(k) P(\kappa^+, \kappa^-). \quad (\text{S-10})$$

The equations (S-1) do simplify as $\mathcal{G}^+(x) = \mathcal{G}^-(x)$ and the phase diagram is independent of the degree distribution $P(\kappa^+, \kappa^-)$. Therefore in this limit we recover Eqs. (2) of the main text that we repeat here for completeness, i.e.,

$$\begin{aligned} S^{(t)} &= 1 - G_1 \left(1 - S^{(t)} p_L^{(t-1)} \right), \\ R^{(t)} &= 1 - G_0 \left(1 - S^{(t)} p_L^{(t-1)} \right), \\ p_L^{(t)} &= p G_0^-(1 - R^{(t)}) \left[1 - G_0^+ \left(1 - R^{(t)} \right) \right]. \end{aligned} \quad (\text{S-11})$$

Here, we have used the simplified definition of the generating functions given by

$$\begin{aligned} G_0(x) &= \sum_k \pi(k) x^k, \\ G_1(x) &= \sum_k \pi(k) \frac{k}{\langle k \rangle} x^{k-1}, \\ G_0^\pm(x) &= \sum_{\kappa_\pm} \hat{P}_\pm(\hat{\kappa}^\pm) x^{\hat{\kappa}^\pm}. \end{aligned} \quad (\text{S-12})$$

As noted in the main text, Eq. (S-11) for the percolation model regulated by triadic interactions can be formally written as the map [52]

$$R^{(t)} = f\left(p_L^{(t-1)}\right), \quad p_L^{(t)} = g_p\left(R^{(t)}\right), \quad (\text{S-13})$$

or combining these two equations as the map

$$R^{(t)} = h_p\left(R^{(t-1)}\right) = f\left(g_p\left(R^{(t-1)}\right)\right). \quad (\text{S-14})$$

The stationary solution $R^{(t)} = R^*$ of this map obeys the equation

$$R^* = h_p(R^*). \quad (\text{S-15})$$

This stationary solution becomes unstable as soon as

$$|J| = 1, \quad (\text{S-16})$$

where

$$J = h'_p(R^*). \quad (\text{S-17})$$

Interestingly, while the value $J = 1$ indicates a discontinuous and hybrid transition, the value $J = -1$ indicates the onset of period-2 oscillations. While we will give a concrete example of this result in the next section, let us here show that the discontinuous transition observed for $J = 1$ is actually hybrid. To this end we indicate with p_c the value of p for which $J = 1$ is satisfied and we consider small variations $\delta p = p - p_c \ll 1$. We indicate the corresponding change in the stationary solution R^* with $\delta R = R^*(p) - R^*(p_c) \ll 1$. Since both $R^*(p)$ and $R^*(p_c) = R_c$ satisfy the stationary Eq. (S-15), assuming without loss of generality that $h_p(R^*)$ is twice differentiable at $R^*(p_c) = R_c > 0$ we can expand this latter equation in δp and δR^* obtaining

$$\delta R = h'_{p_c}(R_c)\delta R + \frac{1}{2}h''_{p_c}(R_c)(\delta R)^2 + \frac{\partial h_{p_c}(R_c)}{\partial p}\delta p. \quad (\text{S-18})$$

Since $h'_{p_c}(R_c) = 1$ this equation reduces to

$$\frac{1}{2}h''_{p_c}(R_c)(\delta R)^2 + \frac{\partial h_{p_c}(R_c)}{\partial p}\delta p = 0, \quad (\text{S-19})$$

from which it is immediate to derive the scaling $\delta R \propto (\delta p)^{1/2}$ as long as $h''_{p_c}(R_c)$ and $\partial h_{p_c}(R_c)/\partial p$ have finite values and opposite sign. Therefore we have shown that

$$R^*(p) - R_c \propto (p - p_c)^{1/2}, \quad (\text{S-20})$$

which establishes that the discontinuous transition is hybrid.

UNCORRELATED POISSON CASE

Theory of regulated percolation

In this section we investigate the instability of the stationary solution in the case of a Poisson structural network of average degree c in which the structural and the regulatory degrees of the nodes are uncorrelated, i.e.,

$$\tilde{P}(k, \kappa^+, \kappa^-) = \pi(k)P(\kappa^+, \kappa^-), \quad (\text{S-21})$$

with

$$\pi(k) = \frac{1}{k!}c^k e^{-c}. \quad (\text{S-22})$$

Additionally we assume that $\hat{\kappa}^+$ and $\hat{\kappa}^-$ are drawn from Poisson distributions with average degree c^+ and c^- respectively, i.e.,

$$\hat{P}_\pm(\hat{\kappa}^\pm) = \frac{1}{\hat{\kappa}^\pm!}(c^\pm)^{\hat{\kappa}^\pm} e^{-c^\pm}. \quad (\text{S-23})$$

Eq. (S-11) for the regulated percolation reduces to

$$\begin{aligned} R^{(t)} &= 1 - e^{-cp_L^{(t-1)} R^{(t)}} \\ p_L^{(t)} &= p \left(1 - e^{-c^+ R^{(t)}} \right) e^{-c^- R^{(t)}}. \end{aligned} \quad (\text{S-24})$$

The first equation can be expressed as a map between $p_L^{(t-1)}$ and $R^{(t)}$, while the second equation can be expressed as a map between $R^{(t)}$ and $p_L^{(t)}$, i.e.,

$$R^{(t)} = f \left(p_L^{(t-1)} \right), \quad p_L^{(t)} = g_p \left(R^{(t)} \right). \quad (\text{S-25})$$

Both equations can be combined in the single map

$$R^{(t)} = h_p \left(R^{(t-1)} \right) = f \left(g_p \left(R^{(t-1)} \right) \right). \quad (\text{S-26})$$

Onset of the instability of the stationary solutions

Regulated percolation on the structural Poisson network admits a stationary steady state when Eqs. (S-24) have the solution $R^{(t)} = R^*$, $p_L^{(t)} = p_L^*$, where R^* and p_L^* satisfy

$$\begin{aligned} R^* &= 1 - e^{-cp_L^* R^*}, \\ p_L^* &= p \left(1 - e^{-c^+ R^*} \right) e^{-c^- R^*}. \end{aligned} \quad (\text{S-27})$$

These equations can be expressed as a single equation

$$R^* = h_p(R^*) = f(g_p(R^*)), \quad (\text{S-28})$$

where the functions $h_p(R)$, $f(p_L)$ and $g_p(R)$ have the same definition as in the previous paragraph. The stationary solution becomes unstable for

$$|J| = |h'_p(R^*)| = \left| \frac{df(g_p(R^*))}{dR^*} \right| = |f'(p_L^*)g'_p(R^*)| = 1, \quad (\text{S-29})$$

where

$$\begin{aligned} f'(p_L^*) &= -\frac{cR^*}{cp_L^* - e^{cp_L^* R^*}}, \\ g'_p(R^*) &= p(c^+ + c^-)e^{-(c^- + c^+)R^*} - c^- p e^{-c^- R^*}. \end{aligned} \quad (\text{S-30})$$

Solving Eq.(S-27) and Eq.(S-29) numerically when $J = 1$ we find the critical line of discontinuous hybrid transitions and when $J = -1$ we find the critical line of the onset of period-2 oscillations of the order parameter $R^{(t)}$.

In Figure S-1 we show graphically the difference between the two types of possible instabilities of the stationary solution $R^* = h(R^*)$. When $J = h'(R^*) = 1$ one observes the discontinuous emergence of a non-zero stationary solution $R^* > 0$. When $J = h'(R^*) = -1$ we observe the onset of period-2 oscillations of the order parameter satisfying the map $R^{(t)} = h(R^{(t-1)})$.

In Figure S-2 we show the obtained critical lines of the onset of period-2 oscillations of the order parameters (blue lines panels (a) and (b)) and for the onset of discontinuous hybrid transitions.

TUNING THE POSITIVE AND NEGATIVE REGULATORY INTERACTIONS

Regulatory percolation in presence of triadic interactions admits two limiting scenarios: the limit $c^- \rightarrow 0$ in which the model includes only positive regulatory interactions and is insensitive to negative regulations, and the limit $c^+ \rightarrow \infty$ in which the role of positive regulatory interactions becomes negligible. In fact if $c^- \rightarrow 0$ then the condition that none of the negative regulators is active is always satisfied. On the contrary if $c_+ \rightarrow \infty$ it becomes sure that at least one of the infinite positive regulators is active, so the role of positive regulators becomes negligible. In Figures S-3 and S-4 we investigate the theoretically predicted orbit diagrams of regulated percolation for

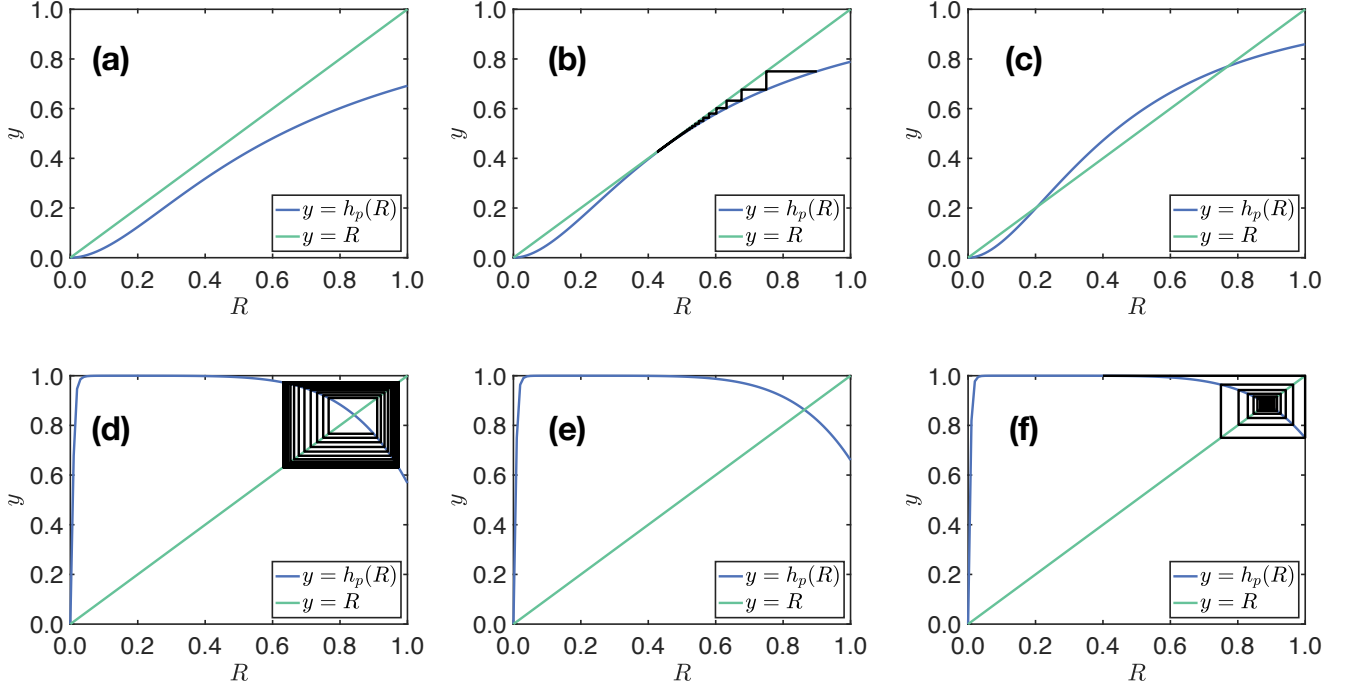


FIG. S-1. The figures show the two different modalities for the onset of the instability of the stable solution of the iterative map $R^{(t)} = h_p(R^{(t-1)})$ for a Poisson network with triadic interactions corresponding to the crossing of the curves $y = h_p(R)$ and $y = R$. In panels (a),(b),and (c) we show the emergence of the discontinuous transition at $p = 0.392$ (panel (b)) on a Poisson network with average degree $c = 4$, and Poisson distribution $\hat{P}^\pm(\hat{\kappa}^\pm)$ with average degrees $c^+ = 4$ and $c^- = 0$ respectively. Panels (a) and (c) show the functions $y = h_p(R)$ and $y = R$ for $p = 0.30$ (below the transition) and $p = 0.50$ (above the transition). Note that in panel (b) the function $y = h(R)$ and the function $y = R$ are tangent to each other at their non-trivial intersection indicating that the non-trivial solution disappears as soon as $p < 0.392$. In panel (d),(e),(f) we show the emergence of 2-cycle at $p = 0.665$ (panel (e)) for a Poisson network with average degree $c = 30$, and Poisson distributions $\hat{P}^\pm(\hat{\kappa}^\pm)$ with average degree $c^+ = 10$ and $c^- = 2.5$ respectively. Panels (d) and (f) show the functions $y = h(R)$ and $y = R$ for $p = 0.60$ (below the transition) and $p = 0.8$ (above the transition) respectively. Note that in panel (e) the function $y = h_p(R)$ displays a derivative -1 leading to the emergence of the 2-limit cycle observed for $p \leq 0.665$. The relative cobweb are shown only for panels (b), (d) and (f) to improve the readability of the figure.

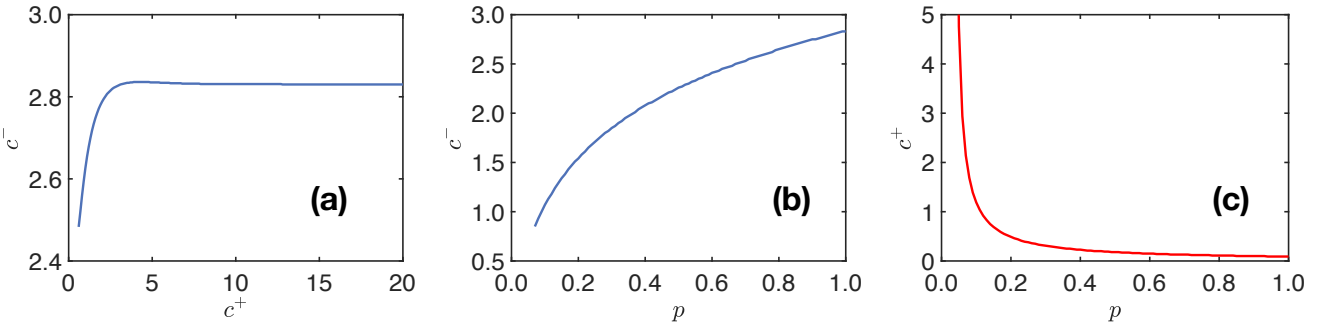


FIG. S-2. (a): Critical line for the onset of period-2 limit cycles for a Poisson network with average degree $c = 30$ and $p = 1$ plotted in plane (c^+, c^-) . (b) Critical line for the onset of period-2 limit cycles for a Poisson network with average degree $c = 30$ and $c^+ = 1000$ plotted in plane (p, c^-) . (c) Critical line for indicating the discontinuous hybrid transition of Poisson network with average degree $c = 30$ and $c^- = 0$ plotted in plane (p, c^+) . In all three cases c^\pm indicate the average degree of the Poisson distribution $\hat{P}_\pm(\hat{\kappa}^\pm)$.

a Poisson structural network and for a scale-free structural network with structural degree uncorrelated with the

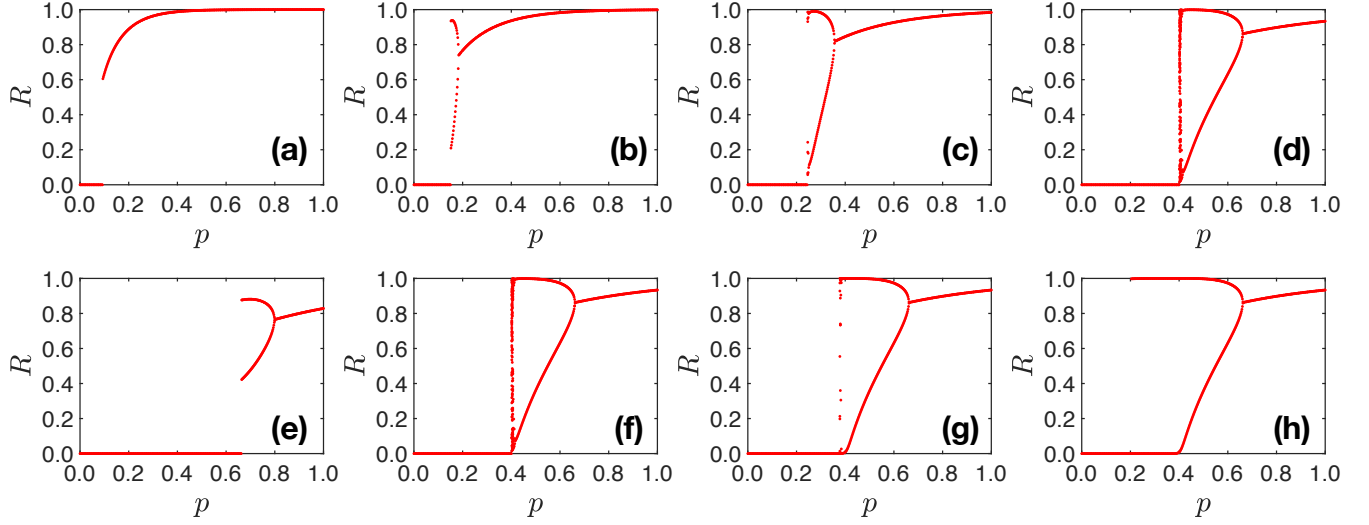


FIG. S-3. Theoretically obtained orbit diagrams of the Poisson structural network with average degree $c = 30$ and uncorrelated structural and regulatory degrees of the nodes. In the first row, $c^+ = 10$, from the left to the right we increase the c^- that $c^- = 1.0$ (a), $c^- = 1.5$ (b), $c^- = 2.0$ (c), $c^- = 2.5$ (d). In the second row, $c^- = 2.5$, from the left to the right we increase the c^+ that $c^+ = 1$ (e), $c^+ = 10$ (f), $c^+ = 1000$ (g), $c^+ = \infty$ (h). In all the panels c^\pm indicate the average degree of the Poisson distribution $\hat{P}_\pm(\hat{\kappa}^\pm)$. All figures are obtained by setting the initial condition $p_L^{(0)} = 0.1$.

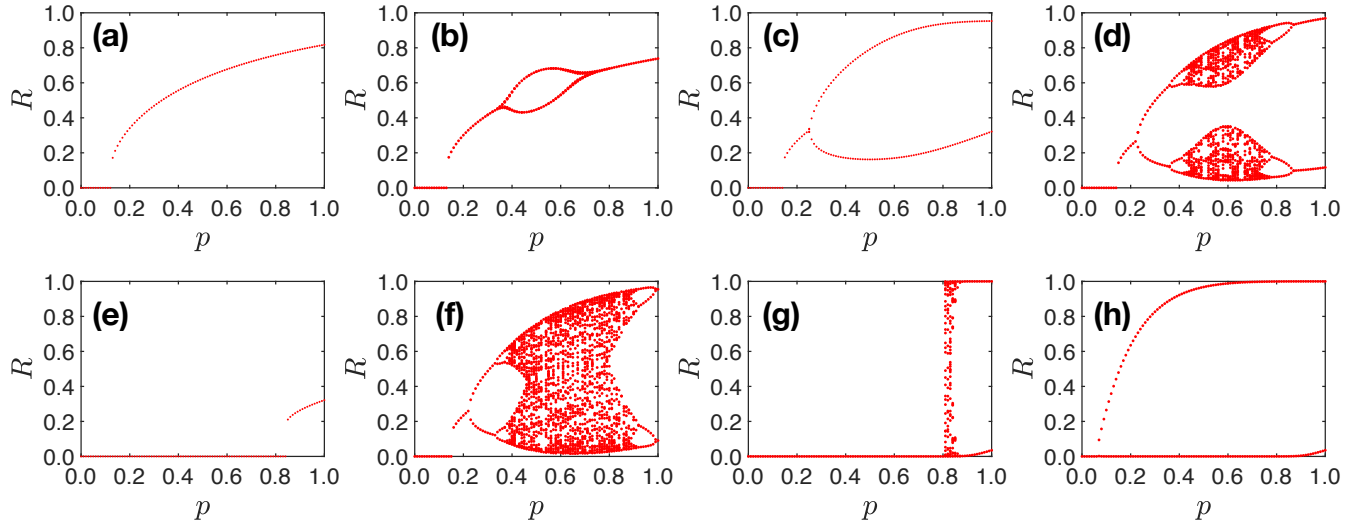


FIG. S-4. Theoretically obtained orbit diagrams of the scale-free structural network with minimum degree $m = 4$, power-law exponent $\gamma = 2.5$, maximum degree $K = 100$ and uncorrelated structural and regulatory degrees of the nodes. In the first row, $c^+ = 10$, from the left to the right we increase the c^- that $c^- = 1.5$ (a), $c^- = 1.9$ (b), $c^- = 2.3$ (c), $c^- = 2.7$ (d). In the second row, $c^- = 2.8$, from the left to the right we increase the c^+ that $c^+ = 1$ (e), $c^+ = 10$ (f), $c^+ = 1000$ (g), $c^+ = \infty$ (h). In all the panels c^\pm indicate the average degree of the Poisson distribution $\hat{P}_\pm(\hat{\kappa}^\pm)$. All figures are obtained by setting the initial condition to $p_L^{(0)} = 0.1$.

regulatory degrees as a function of the average degrees c^+ and c^- of the Poisson distributions $\hat{P}_\pm(\hat{\kappa}^\pm)$. In absence of negative regulators, i.e., $c^- \rightarrow 0$, we observe a discontinuous hybrid transition in both cases (although displaying a smaller discontinuity for the scale-free structural network). For $c^+ = \infty$, we observe period-2 oscillations in the case of the Poisson network and a single stable solution in the scale-free case. In both cases, we observe chaos only in presence of both positive and negative regulatory interactions.

COMPARISON BETWEEN THE THEORY AND THE MONTE CARLO SIMULATIONS

In the main text, we have studied the period-doubling cascade and the route to chaos of regulated percolation as a function of the probability p that a link is intact when all the regulatory interactions are satisfied. However, here we show that the period-doubling cascade and the route to chaos can also be observed for fixed value of p as a function of the average degree c^- of the Poisson distribution $\hat{P}_-(\hat{\kappa}^-)$ in the case of uncorrelated structural and regulatory degrees of the nodes. In Figures *S* – 5 and *S* – 6, we show the theoretically obtained orbit diagram as a function of c^- for a Poisson and for a scale-free network respectively and we compare the theoretical predictions with Monte Carlo simulations of regulated percolation for different values of c^- finding very good agreement.

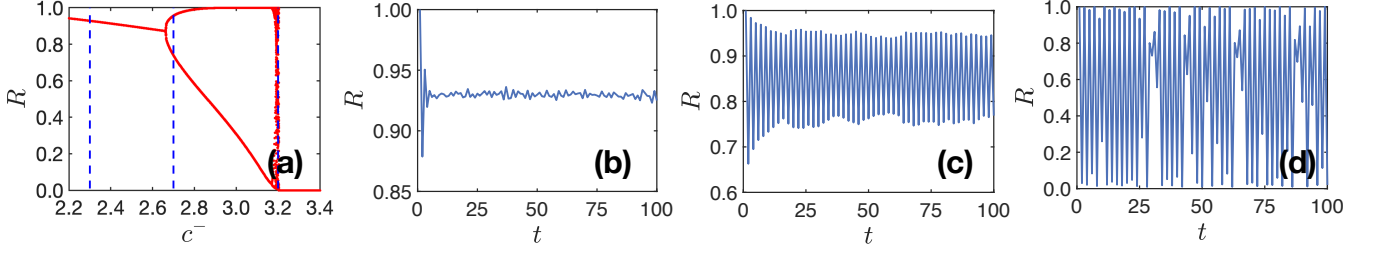


FIG. S-5. Theoretical obtained orbit diagram at fixed value $p = 0.8$ for the Poisson structural network, with average degree $c = 30$, uncorrelated structural and regulatory degree, Poisson distributed $\hat{\kappa}^\pm$ with average $\langle \hat{\kappa}^+ \rangle = c^+ = 10$ and $\langle \hat{\kappa}^+ \rangle = c^-$. The tree blue lines in panel (a) indicate $c^- = 2.3$, $c^- = 2.7$ and $c^- = 3.2$. The corresponding Monte Carlo simulations on networks of $N = 10^4$ are shown in panel (b),(c) and (d). All figures are obtained with an initial condition $p_L^{(0)} = 0.1$.

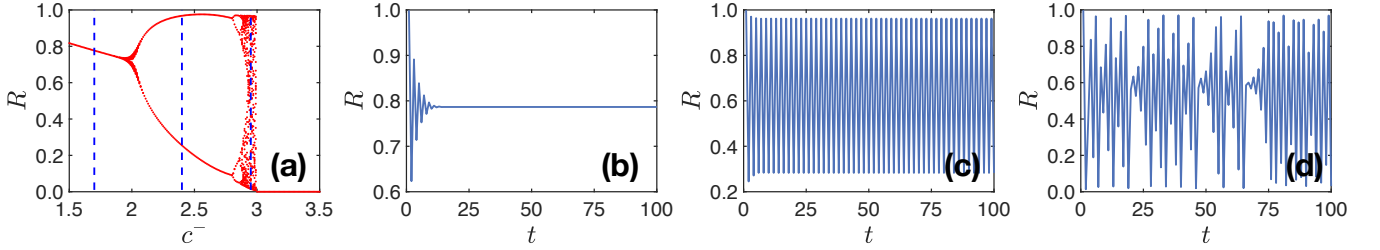


FIG. S-6. Theoretical obtained orbit diagram at fixed value $p = 1$ for the scale-free structural network, with minimum degree $m = 4$, maximum degree $K = 100$, power-law exponent $\gamma = 2.5$. The nodes have uncorrelated structural and regulatory degrees, and the distribution of $\hat{\kappa}^\pm$ is Poisson with average $\langle \hat{\kappa}^+ \rangle = c^+ = 10$ and $\langle \hat{\kappa}^+ \rangle = c^-$. The tree blue lines in panel (a) indicate $c^- = 1.7$, $c^- = 2.4$ and $c^- = 2.95$. The corresponding Monte Carlo simulations on a network of $N = 10^4$ nodes are shown in panel (b) (c) and (d). All figures are obtained with an initial condition $p_L^{(0)} = 0.1$.

In order to show furthermore the agreement between the theoretical expectation and the Monte Carlo simulations in Figure *S* – 7 we compare the amplitude of the period-2 oscillations of the order parameter obtained with the Monte Carlo simulations with the predicted amplitude of the period-2 oscillations of the order parameter in a region of phase space where only period two oscillations are predicted. We find excellent agreement for both Poisson structural networks and scale-free structural networks with structural degree of the nodes uncorrelated with the regulatory degrees of the nodes.

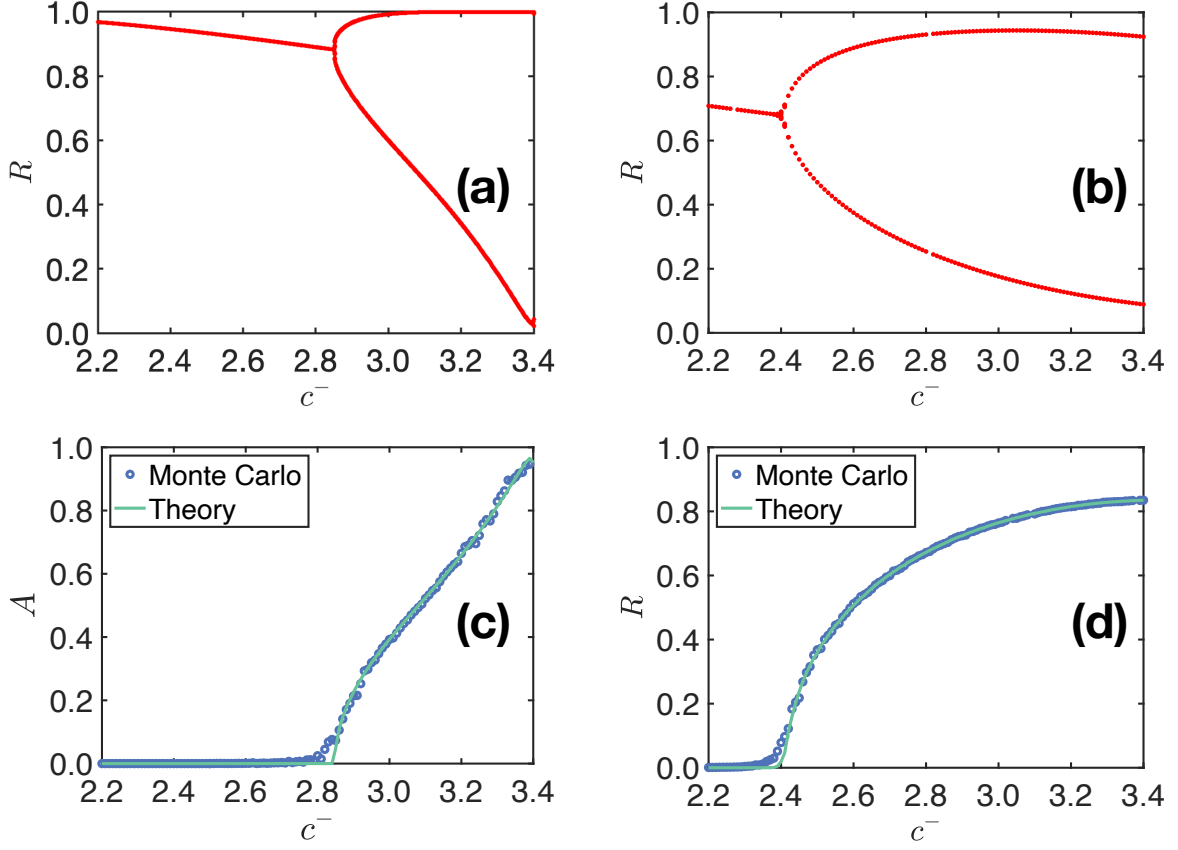


FIG. S-7. In panel (a) and (b) we show the theoretically obtained orbit diagram of regulated percolation on a Poisson network (a) and a scale-free network (b) for $p = 1$ as a function of c^- indicating the average degree of the Poisson distribution $\hat{P}_-(\hat{\kappa}^-)$. In panel (c) and (d), we plot the amplitude $A = \langle |R^{(t)} - R^{(t-1)}| \rangle$ of the period 2 oscillations of the order parameter obtained by Monte Carlo simulations (blue circles) of regulated percolation as a function of the average degree c^- (panel (c) refers to the same Poisson network as panel (a) and panel (d) refers to the same and scale-free network as panel (b)). The theoretical prediction for the amplitude A are indicated with a green solid line in panels (c) and (d). The Poisson network (panels (a) and (c)) has average structural degree $c = 30$ and average degree of the Poisson distribution $\hat{P}_+(\hat{\kappa}^+)$ equal to $c^+ = 10$. The scale-free network (panels (a) and (c)) has minimum degree $m = 4$, power-law exponent $\gamma = 2.5$ and average degree of the Poisson distribution $\hat{P}_+(\hat{\kappa}^+)$ equal to $c^+ = 10$. The Monte Carlo simulations are conducted on networks of $N = 10^4$ nodes; the amplitude A is obtained by averaging over 10 network realizations.